Charge exchange, scattering, and transfer reactions for $^{9}Be+^{6}Li$ and analysis of $^{14}C(^{6}Li,^{6}He)$

J. Cook* and K. W. Kemper
Department of Physics, Florida State University, Tallahassee, Florida 32306
(Received 26 December 1984)

Angular distributions for the $^{9}Be(^{6}Li,^{6}He)$ charge exchange reaction, $^{9}Be(^{6}Li,^{6}Li)$ elastic and inelastic scattering, and the $^{9}Be(^{6}Li,^{7}Li)$ transfer reaction have been measured at $E=32$ MeV. Limited measurements at 36 MeV showed no change in the cross sections at this energy compared with those at 32 MeV. Coupled channels calculations are necessary to describe the inelastic scattering data to the ^{9}Be, 2.43 MeV, $\frac{5}{2}^{-}$ state. The deformation length obtained is in good agreement with the electron scattering value. A microscopic analysis of the charge exchange reaction shows that the M3Y interaction gives a good description of the ^{9}Be ground state to ^{9}B ground state transition, but underpredicts the cross section to the ^{9}B, 2.36 MeV, $\frac{5}{2}^{-}$ state by a factor of 3. The same calculations carried out for previously reported $^{14}C(^{6}Li,^{6}He)$ data reproduce the magnitude of the data provided that Visscher-Ferrell densities are used for the ^{14}C to ^{14}N transition. The results of finite range distorted-wave Born approximation calculations for $^{9}Be(^{6}Li,^{7}Li_{0,1})^{8}Be_{0}$ show the neutron pickup spectroscopic factors to be in good agreement with the Cohen-Kurath calculations.

I. INTRODUCTION

A recent[1] microscopic analysis of the $^{16}O(^{7}Li,^{7}Be)^{16}N$ reaction was unsuccessful in reproducing the magnitude of the measured cross sections. Since the structure of the states in ^{16}N chosen for the analysis is well known, this analysis showed that either the effective interaction used was incorrect or that multistep processes dominated the reaction, or that both possibilities were true. In contrast, recent analyses of the $(^{6}Li,^{6}He)$ reaction seem to indicate that this reaction has a large quasi-elastic component. While single-step forbidden reactions are observed,[2,3] they tend to be about a factor of 5-10 weaker than allowed transitions. The strongest evidence to date for a single-step interpretation of the allowed $(^{6}Li,^{6}He)$ reactions is the correlation between known Gamow-Teller strengths and the $l=0$ component of the $(^{6}Li,^{6}He)$ cross sections.[4] For the higher l transfers microscopic distorted-wave Born approximation (DWBA) calculations[5,6] give a good description of the data, but independent confirmation of the calculations is more difficult. For these transitions good agreement has been found for the extracted isovector spin-flip interaction strength in $(^{6}Li,^{6}He)$ and low energy (p,p') and (p,n) reactions.[7] This latter comparison is made difficult because of the rapid energy dependence and target mass dependence in this interaction for proton energies less than 25 MeV.[8]

In this work, new data for the $^{9}Be(^{6}Li,^{6}He)^{9}B$ reaction are presented, with microscopic DWBA calculations for this reaction and for the more intensely studied $^{14}C(^{6}Li,^{6}He)^{14}N$ reaction.[4,9] The same interaction was used in these calculations as in the unsuccessful $(^{7}Li,^{7}Be)$ study. The central part of this interaction (M3Y) has successfully described the elastic and inelastic scattering of light heavy ions. The elastic scattering data for $^{6}Li+^{9}Be$ were analyzed in terms of the optical model, and both DWBA and coupled channels analyses of the inelastic data were carried out. The transfer data were compared with exact finite-range DWBA calculations to determine the neutron spectroscopic factors for the $^{9}Be(^{6}Li,^{7}Li)^{8}Be$ reactions.

II. EXPERIMENTAL METHODS

The proton and ^{6}Li beams used in the measurements presented here were produced in an inverted sputter source and accelerated in the Florida State University (FSU) Super FN tandem Van de Graaff. The scattered particles were detected in two $\Delta E\times E$ counter telescopes consisting of 40 μm Si surface barrier detectors and 4 mm Si(Li) detectors. A Si surface barrier detector was used as a monitor detector throughout the measurements. This detector provided a continuous check on the target condition and beam integration. Standard electronics were used to provide amplified signals for input to the data collection computer system. Particle identification was performed on line with this computer so that the yields for the ^{6}Li, ^{7}Li, and ^{6}He particle groups could be extracted during the data runs. This proved useful in determining when sufficient yields were present in the individual particle groups to provide a reliable reaction-to-reaction cross section.

The ^{9}Be targets used were self-supporting and had thicknesses of 84 $\mu g/cm^{2}$. The product of target thickness times solid angle, necessary to obtain the absolute cross sections for the ^{6}Li-induced studies, was found by scattering 11.9 and 14 MeV protons from the targets and comparing the extracted yields to previously reported cross sections[10] in the laboratory angular range of 85°—110°. The absolute error in the ^{6}Li-induced scattering and reaction results presented here is estimated to be 12%. The primary contribution to this error arises from the ac-

curacy to which the elastic and inelastic proton cross sections can be read from the published graphs of the data.

Detailed angular distribution data at $E(^6\text{Li})=32$ MeV were taken for $^6\text{Li}+^9\text{Be}_{0,1}$, $^9\text{Be}(^6\text{Li},^7\text{Li}_{0,1})^8\text{Be}_{0,1}$, and $^9\text{Be}(^6\text{Li},^6\text{He})^9\text{Be}_{0,1}$, where the subscript 0 or 1 refers to the nucleus in its ground or first excited state, respectively. Typical spectra for all three systems studied are shown in Fig. 1. The relative population between the ground and first excited states in ^{9}B is the same as that reported previously[11] for a bombarding energy of 31 MeV. To make certain that the $^9\text{Be}(^6\text{Li},^6\text{He})$ cross section is not a rapidly changing function of bombarding energy, five angles were repeated at an energy of 36 MeV. The cross sections were the same, within the statistical uncertainties as those at 32 MeV.

III. DATA ANALYSIS

A. Elastic scattering

The elastic scattering data were analyzed with the optical model (OM) using Woods-Saxon nuclear potentials and a Coulomb potential due to a uniformly charged sphere. Starting parameters were taken from a study[12] of $^6\text{Li}+^{12}\text{C}$ scattering at 30 MeV. This potential provided a reasonable description of the 32 MeV $^6\text{Li}+^9\text{Be}$ elastic scattering data. The potential parameters were then optimized using the optical model code HERMES (Ref. 13) to best fit the data. The main changes were a decrease in the depth of the imaginary potential, and an increase in the imaginary radius parameter. The other parameters only changed by small amounts. The final optical potential parameters are given in Table I and the fit to the data is shown as the full line in Fig. 1. The overall quality of the fit is good. However, the magnitudes of the maxima at $\theta\approx 12°$ and $\theta\approx 18°$ are underpredicted, and the second maximum is shifted in phase by about 2°. It was not possible to adjust the potential to rectify these problems. Different starting parameters were also tried, without any improvement except sometimes increasing the magnitude of the second maximum at the expense of reducing the magnitude of the third.

B. Inelastic scattering

Data for the inelastic excitation of the $\frac{5}{2}^-$ 2.43 MeV excited state of ^{9}Be were analyzed with the computer code CHUCK3 (Ref. 15) using the DWBA and coupled-channels (CC) techniques. The $\frac{3}{2}^-$ ground state and $\frac{5}{2}^-$ 2.43 MeV state of ^{9}Be were assumed to be members of a $K=\frac{3}{2}$ rotational band, and deformed Woods-Saxon form factors were used for the $\frac{3}{2}^-\rightarrow\frac{5}{2}^-$ transition and, in the CC calculations, the reorientation terms in the two states were included. Only $l=2$ couplings were considered, and Coulomb excitation was included. The same deformation length δ_2 was used for real and imaginary nuclear terms and for Coulomb excitation.

The DWBA prediction for the $\frac{5}{2}^-$ state is shown as the solid line in Fig. 2. A deformation length of $\delta_2=1.7$ fm was determined by normalizing the DWBA prediction to the first maximum in the experimental data at $\theta\approx 16°$.

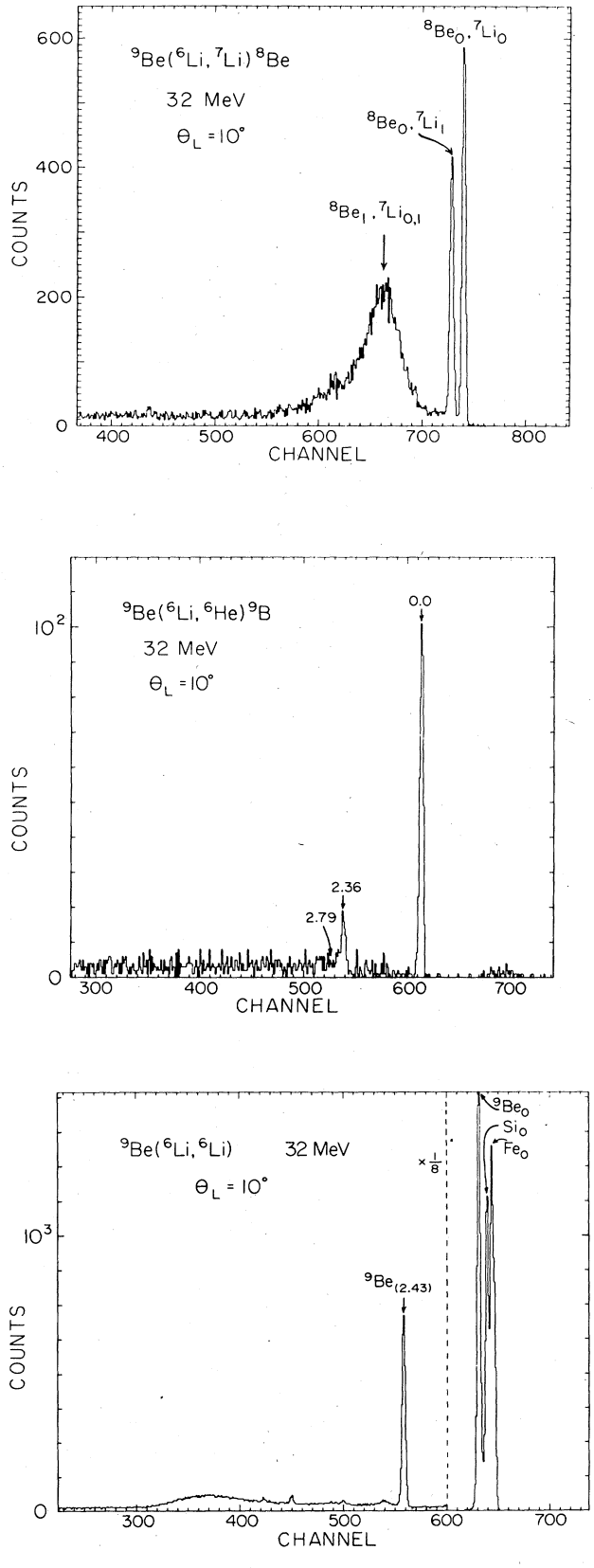

FIG. 1. Typical spectra for the reactions studied.

TABLE I. Optical model parameters.

System	E (MeV)	Analysis	V_0 (MeV)	r_R^a (fm)	a_R (fm)	W_0 (MeV)	r_I^a (fm)	a_I (fm)	r_c^a (fm)	δ_2 (fm)	Ref.
^{6}Li+^{9}Be	32	OM	174	1.22	0.75	5.84	2.81	0.63	2.34		Present work
^{6}Li+^{9}Be	32	DWBA	174	1.22	0.75	5.84	2.81	0.63	2.34	1.7	Present work
^{6}Li+^{9}Be	32	CC	140	1.22	0.83	6.00	2.81	0.60	2.34	1.9	Present work
^{6}Li+^{14}C	34	OM	186	1.11	0.83	7.74	2.21	0.69	2.19		12
^{6}Li+^{14}C	62	OM	174	1.21	0.79	17.2	2.16	0.62	2.19		12
^{7}Li+^{9}Be	34	OM	173	1.19	0.78	8.90	2.52	0.92	1.78		14

[a] $R_x = r_x A_T^{1/3}$.

The DWBA prediction overestimates the data at larger angles, suggesting the presence of strong coupling effects. This was confirmed in the CC calculations, where the predicted cross sections decreased as soon as the $\frac{5}{2}^-$ state was allowed to couple back to the ground state. The phasing of the elastic cross sections was now incorrect, requiring a reduction in the strength of the real potential. The best fit was then obtained by gridding on the other parameters. Only small changes were required and the final parameters are given in Table I. A deformation length of $\delta_2 = 1.9$ fm, used for both the transition and reorientation form factors, was found from the CC analysis. Both the elastic and inelastic data were then described reasonably well.

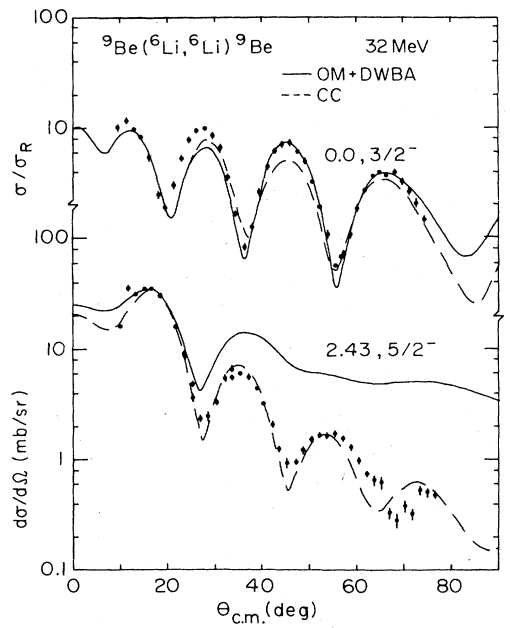

FIG. 2. Data for the elastic scattering of ^{6}Li+^{9}Be at 32 MeV, and for the inelastic excitation of the $\frac{5}{2}^-$ 2.43 MeV state of ^{9}Be. The full lines are the results of optical model and DWBA calculations. The dashed lines correspond to coupled channels calculations. Woods-Saxon potentials and form factors were used throughout, with parameters given in Table I.

If a uniformly charged distribution for ^{9}Be is assumed, then a deformation length of $\delta_2 = 1.7 \pm 0.1$ fm is found from the spectroscopic quadrupole moment[16] of $Q_2 = 4.9 \pm 0.3$ e fm^2, and a value[17] of $\delta_2 = 1.97 \pm 0.08$ fm from the $B(E2) = 45.7 \pm 3.5$ e^2fm^4 value[6] between the $\frac{3}{2}^-$ and $\frac{5}{2}^-$ states. The difference between these two values reflects the fact that ^{9}Be is not a good rigid rotor nucleus. The deformation length found from the present calculations is determined from the extent of the coupling between the $\frac{3}{2}^-$ and $\frac{5}{2}^-$ states, and thus the value of 1.9 fm used in the CC calculations is in good agreement with that extracted from the $B(E2)$ value.

C. Charge exchange

The ^{9}Be(^{6}Li,^{6}He)^{9}B charge exchange data leading to the $\frac{3}{2}^-$ ground state and $\frac{5}{2}^-$ 2.36 MeV states of ^{9}B were analyzed in the DWBA using a microscopic form factor. These states are the isobaric analogs of the $\frac{3}{2}^-$ ground state and $\frac{5}{2}^-$ 2.43 MeV states of ^{9}Be. This reaction might be expected to be a good candidate for a direct single-step charge exchange reaction since ^{9}Be has the structure of a neutron loosely bound to a core consisting of two alpha clusters, whereas ^{9}B has a proton loosely bound to the same core. The optical model parameters found in Sec. III A were used for generating the distorted waves for both ^{6}Li+^{9}Be and for ^{6}He+^{9}B. The microscopic form factor was generated by convoluting the necessary parts of the M3Y effective nucleon-nucleon interaction[18] with harmonic-oscillator transition densities for ^{6}Li$\rightarrow$^{6}He and ^{9}Be$\rightarrow$^{9}B. The formalism has been presented in a previous paper,[1] and in that notation, the spectroscopic amplitudes $S^J_{TM}(j_f j_i)$ required for calculating the transition densities are tabulated in Table II for Cohen-Kurath[19] wave functions. On the basis of Ref. 20, an oscillator parameter for $\alpha = 0.505$ fm^{-1} was used for the $1p$ nucleons in ^{6}Li. The Cohen-Kurath wave functions reproduce[20] reasonably well, for small momentum transfers, inelastic electron scattering to the 3.65 MeV 0^+ $T=1$ state of ^{6}Li (the isobaric analog of the ^{6}He ground state), while overestimating the experimental β-decay matrix element (Table III and Ref. 20). This is a measure of the $l=0$ transition strength between the 1^+ $T=0$ and 0^+ $T=1$ states in the mass 6 system, and is dominant compared with the $l=2$

TABLE II. Spectroscopic amplitudes $S^J_{TM_T}(j_f j_i)$ for the charge exchange calculations.

Transition	Model[a]	α (fm^{-1})	J	$S^J_{TM_T}(j_f j_i)$ $1p_{1/2}$ $1p^{-1}_{1/2}$	$1p_{3/2}$ $1p^{-1}_{1/2}$	$1p_{1/2}$ $1p^{-1}_{3/2}$	$1p_{3/2}$ $1p^{-1}_{3/2}$
^{6}Li(g.s.)→^{6}He(g.s.)	CK	0.505	1	0.101	−0.965	0.648	0.936
^{9}Be(g.s.)→^{9}B(g.s.)	CK	0.602	0	0.043	0.0	0.0	1.370
			1	−0.108	−0.110	−0.078	0.909
			2	0.0	0.170	−0.120	0.293
			3	0.0	0.0	0.0	1.066
^{9}Be(g.s.)→^{9}B($\frac{5}{2}^-$, 2.36 MeV)	CK	0.602	1	0.069	0.402	0.091	0.721
			2	0.0	−0.131	0.226	0.641
			3	0.0	0.0	0.0	−0.382
^{14}C(g.s.)→^{14}N(g.s.)	CK	0.612	1	−1.030	0.219	−0.048	0.036
^{14}C(g.s.)→^{14}N(g.s.)	VF	0.612	1	−1.035	0.405	−0.052	−0.035

[a]CK denotes the wave functions of Cohen and Kurath (Ref. 19); VF denotes the wave functions of Visscher and Ferrell (Ref. 25).

strength. The magnetic moment of ^{6}Li and the $B(M1)$ value for the ground state to 3.65 MeV 0^+ $T=1$ state are underestimated. Thus there may be some deficiencies in the Cohen-Kurath transition density for ^{6}Li→^{6}He, but overall these wave functions produce a reasonable description of the mass 6 system.[20] An oscillator parameter of $\alpha=0.602$ fm^{-1} was chosen for ^{9}Be to best fit the ground state charge form factor.[24]

Figure 3 shows the results of the DWBA calculations described above. Shown separately are the cross sections calculated using the central part of the interaction only, the tensor part of the interaction only, and both the central and tensor parts. The predicted cross sections have been multiplied by a factor N so that those calculated with both the central and tensor parts of the interaction best describe the data. This number provides some indication as to how well the reaction is described in terms of the wave functions, interaction, and mechanism involved. In particular, for the case here, where realistic and well-tested wave functions and interactions are being employed, a value of N close to unity should indicate that the reaction is well described as being of direct single-step charge exchange type. The normalizations required are $N=1.1$ for transitions to the ^{9}B ground state, and $N=3.0$ to the $\frac{5}{2}^-$ 2.36 MeV state of ^{9}B. Thus the ground-state transition is likely to be a single-step reaction, whereas some multistep routes may be important for the excited state. In Sec. III, it was found that the $\frac{3}{2}^-$ and $\frac{5}{2}^-$ states of ^{9}Be are strongly coupled, and a coupled channels calculation is probably required in which the $\frac{3}{2}^-$ and $\frac{5}{2}^-$ states of ^{9}Be are coupled, as well as the $\frac{3}{2}^-$ and $\frac{5}{2}^-$ states of ^{9}B, together with the charge-exchange routes between them. For both states it is found that the central part of the interaction produces the largest contribution to the cross sections, with the tensor interaction filling in the minima.

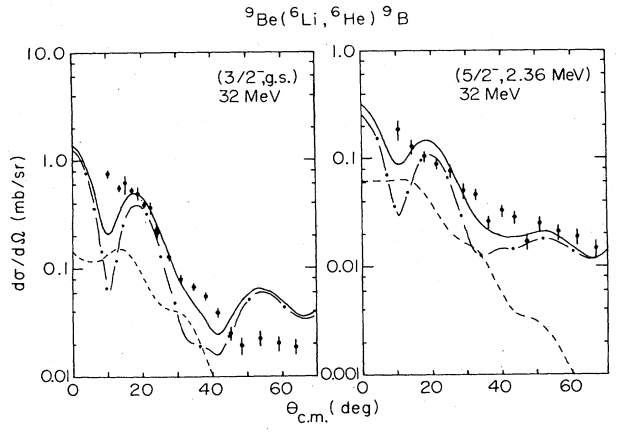

FIG. 3. DWBA predictions for the reaction ^{9}Be(^{6}Li,^{6}He)^{9}B at 32 MeV compared with experimental data. The calculations used microscopic form factors calculated with Cohen-Kurath wave functions. The three curves correspond to central and tensor interactions (full lines), only central interaction (dot-dashed lines), and only tensor interaction (dashed lines). The predictions have been multiplied by 1.1 and 3.0 for the $\frac{3}{2}^-$ and $\frac{5}{2}^-$ states, respectively.

Microscopic DWBA calculations were also made for previously published data for the ^{14}C(^{6}Li,^{6}He)^{14}N charge exchange reaction at 34 (Ref. 9) and 62 (Ref. 4) MeV, for which extensive studies have previously concluded that it proceeds in a single step. Optical potentials for ^{6}Li+^{12}C from Ref. 12 were used for generating the distorted waves. Initially, Cohen-Kurath wave functions were used for ^{14}C→^{14}N with an oscillator parameter of $\alpha=0.612$ fm^{-1} (to obtain the correct rms radius for the ground state). The spectroscopic amplitudes are listed in Table II. As can be seen from Table III, these wave functions have too large an $l=0$ component since they overestimate the

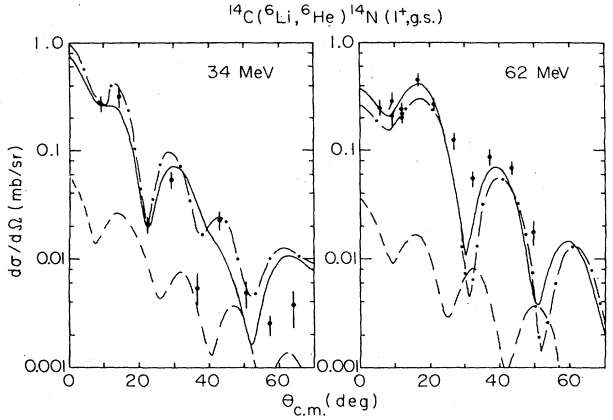

FIG. 4. DWBA predictions for the reaction ^{14}C(^{6}Li,^{6}He)^{14}N at 34 and 62 MeV compared with the experimental data of Refs. 4 and 9. The calculations used microscopic form factors calculated with Cohen-Kurath wave functions. The three curves correspond to central and tensor interactions (full lines), only central interaction (dot-dashed lines), and only tensor interaction (dashed lines). The predictions have been multiplied by 1.8.

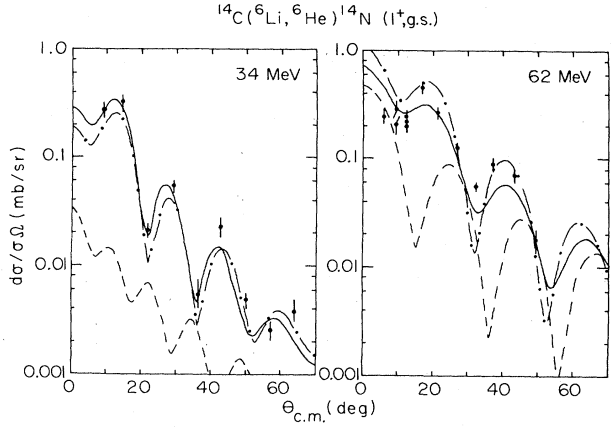

FIG. 5. The same as Fig. 3, but using Visscher-Ferrell wave functions for ^{14}C→^{14}N. The predictions have been multiplied by 1.0.

β-decay matrix element for ^{14}C→^{14}N by several orders of magnitude. They should not, therefore, be expected to describe the reaction data very well. This is confirmed by the calculations which are illustrated in Fig. 4. At both energies the angular distributions are not described well and a normalization of $N=1.8$ has to be applied to the calculated cross sections. In contrast, calculations, shown in Fig. 5, using the wave functions of Visscher and Ferrell[25] for ^{14}C and ^{14}N reproduce the angular distribution well at both energies with $N=1.0$. The dominant contribution again comes from the central interaction. The transition density using the Visscher-Ferrell wave functions has a much smaller $l=2$ component than the Cohen-Kurath wave functions, and is in fair agreement with the measured β-decay matrix element (Table III).

It is therefore concluded that the ^{9}Be(^{6}Li,^{6}He)^{9}B and ^{14}C(^{6}Li,^{6}He)^{14}N reactions leading to the ground states of ^{9}B and ^{14}N are well described by microscopic DWBA calculations employing the M3Y effective nucleon-nucleon interaction,[18] Cohen-Kurath[19] transition densities for ^{6}Li→^{6}He and ^{9}Be→^{9}B, and Visscher-Ferrell[25] transition densities for ^{14}C→^{14}N. Furthermore, since the correct magnitude is obtained for the cross sections without any additional normalization, these reactions most probably proceed through a single step.

D. Neutron stripping

In Sec. II, data were reported for the neutron stripping reaction ^{9}Be(^{6}Li,^{7}Li)^{8}Be with:

(i) ^{7}Li and ^{8}Be both in their ground states,

(ii) ^{7}Li in its $\frac{1}{2}^{-}$ 0.478 MeV first excited state and ^{8}Be in its ground state, and

(iii) ^{8}Be in its 3.04 MeV first excited state and ^{7}Li in both its ground and first excited states.

Finite-range DWBA calculations for the first two angular distributions were made using the code DWUCK5.[26] No calculations were made for the third angular distribution since the neutron in this case is unbound. The ^{6}Li+^{9}Be optical potential listed in Table I was used to generate the distorted waves in both the ^{6}Li+^{9}Be and ^{7}Li+^{8}Be channels. The bound state wave functions were obtained as the

TABLE III. β-decay GT matrix elements.

Reaction	$\langle GT\rangle^{2a}_{exp}$	Model[d]	$\langle GT\rangle^{2}_{th}$
^{6}He(g.s.)$\xrightarrow{\beta^-}$^{6}Li(g.s.)	5.09[b]	CK	5.52
^{14}C(g.s.)$\xrightarrow{\beta^-}$^{14}N(g.s.)	3.99×10^{-6}[c]	CK	0.14
		VF	3.42×10^{-7}

[a]Extracted from logft values using $\langle F\rangle^2+1.4\langle GT\rangle^2=6120/ft$ from Ref. 21.
[b]Reference 22.
[c]Reference 23.
[d]CK denotes the wave functions of Cohen and Kurath (Ref. 19); VF denotes the wave functions of Visscher and Ferrell (Ref. 25).

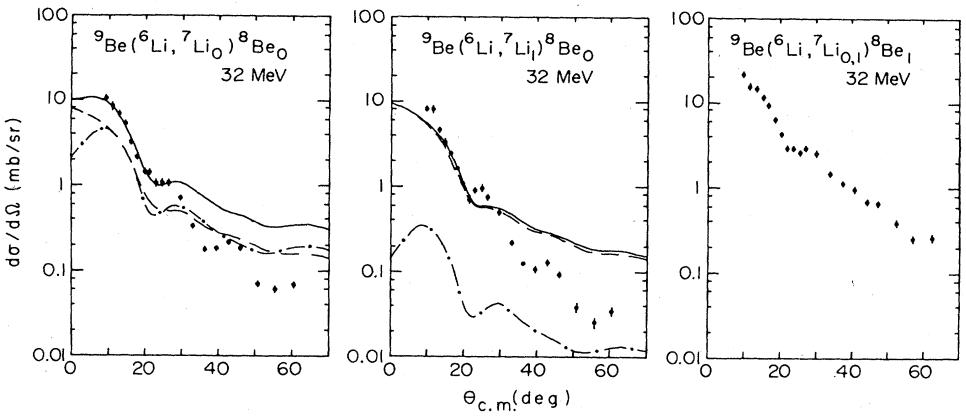

FIG. 6. Finite range DWBA predictions for the reaction ^{9}Be(^{6}Li,^{7}Li)^{8}Be at 32 MeV. The three curves correspond to total cross section (full lines), $1p_{3/2}$ contribution (dashed lines), and $1p_{1/2}$ contribution (dot-dashed lines). The predictions have been multiplied by 0.8.

solution to a Woods-Saxon potential well of geometry $R_0 = 1.25A^{1/3}$ fm and $a_0 = 0.65$ fm with the depth varied to give the correct binding energy. Cohen-Kurath[19] spectroscopic factors were used and are tabulated in Table IV. As can be seen in Fig. 6, the experimental data are well described forward of 30° for ^{7}Li in its ground or first excited states if the predicted cross sections are multiplied by $N = 0.8$. In the former case, transfers to the $1p_{3/2}$ and $1p_{1/2}$ orbitals in ^{7}Li have similar magnitude and shape (except for $\theta < 5°$), but in the latter case the reaction is completely dominated by transfer to the $1p_{3/2}$ orbital. The predictions are greater in magnitude than the data for angles in excess of 30°; this may indicate that channel coupling effects need to be included in coupled-channel Born approximation (CCBA) or coupled reaction channel (CRC) calculations. At present, we do not have the necessary codes to do this with the particle transfer calculated in finite range. Calculations were also made using the potential for ^{7}Li+^{9}Be at 34 MeV from Ref. 14 in the ^{7}Li+^{8}Be channel. The predicted angular distributions had the same shapes as before, but fitted the data with a normalization of $N = 1.0$.

IV. CONCLUSIONS

Angular distributions have been measured for ^{6}Li+^{9}Be elastic scattering at 32 MeV and for the inelastic excitation of the $\frac{5}{2}^-$ 2.43 MeV state of ^{9}Be. The elastic scattering data were well described using the optical model. The $\frac{3}{2}^-$ ground and $\frac{5}{2}^-$ 2.43 MeV states of ^{9}Be were found to be strongly coupled, and coupled channels calculations were necessary to describe the inelastic data. The quadrupole deformation length extracted was in agreement with that found from the quadrupole moment and the $B(E2)$ value for ^{9}Be.

^{9}Be(^{6}Li,^{6}He)^{9}B charge exchange data were also measured at 32 MeV leading to the $\frac{3}{2}^-$ ground state and $\frac{5}{2}^-$ 2.36 MeV states of ^{9}B. The data were analyzed in the DWBA using a microscopic form factor calculated from the central and tensor parts of the M3Y effective nucleon-nucleon interaction and Cohen-Kurath transition densities. The angular distributions were well described in shape, and also in magnitude for the ground state. However, a normalization of 3.0 was required for the $\frac{5}{2}^-$ state, indicating a deficiency in the reaction model or the wave function of this state. Calculations were also made for previously published data for ^{14}C(^{6}Li,^{6}He)^{14}N at 34 and 62 MeV. These data were well described using Visscher-Ferrell wave functions for ^{14}C and ^{14}N, but not with Cohen-Kurath wave functions. These results suggest that the ^{9}Be(^{6}Li,^{6}He)^{9}B and ^{14}C(^{6}Li,^{6}He)^{14}N reactions populating the ground states are good candidates for single-step charge exchange reactions.

Concurrently, data were also measured for the ^{9}Be(^{6}Li,^{7}Li)^{8}Be neutron stripping reaction and were well

TABLE IV. Spectroscopic factors for the neutron pickup reaction ^{9}Be(^{6}Li,^{7}Li)^{8}Be using the wave functions of Cohen and Kurath (Ref. 19).

System	Orbital	C^2S
^{6}Li(g.s.)⊕n→^{7}Li(g.s.)	$1p_{3/2}$	0.431
	$1p_{1/2}$	0.289
^{6}Li(g.s.)⊕n→^{7}Li($\frac{1}{2}^-$,0.478 MeV)	$1p_{3/2}$	0.855
	$1p_{1/2}$	0.039
^{9}Be(g.s.)→^{8}Be(g.s.)⊕n	$1p_{3/2}$	0.580

described by finite-range DWBA calculations employing Cohen-Kurath spectroscopic factors.

Taken together, these results show that the Cohen-Kurath wave functions are reasonable for the mass 6 and 9 systems, but are deficient for mass 14, where the wave functions of Visscher and Ferrell are more appropriate. The (^{6}Li,^{6}He) reaction is dominated by the $S=1$, $T=1$ central part of the interaction, and, further assuming that for the target nuclei ^{9}Be and ^{14}C this reaction proceeds in a single step, the present results show that this component of the force is of correct magnitude.

ACKNOWLEDGMENTS

The authors would like to acknowledge the aid of J. A. Carr, D. P. Sanderson, and S. Van Verst in this work. We also gratefully acknowledge the support of this work by the National Science Foundation and the State of Florida.

*Present address: Department of Physics, University of Petroleum and Minerals, Dhahran, Saudi Arabia.

[1]J. Cook, K. W. Kemper, P. V. Drumm, L. K. Fifield, M. A. C. Hotchkis, T. R. Ophel, and C. L. Woods, Phys. Rev. C **30**, 1538 (1984).

[2]H. H. Duhm, N. Ueta, W. Heinecke, H. Hafner, H. Homeyer, and P. D. Kunz, Phys. Lett. **38B**, 306 (1972).

[3]W. R. Wharton and P. T. Debevec, Phys. Rev. C **11**, 1963 (1975).

[4]C. D. Goodman, W. R. Wharton, and D. C. Hensley, Phys. Lett. **64B**, 417 (1976); W. R. Wharton, C. D. Goodman, and D. C. Hensley, Phys. Rev. C **22**, 1138 (1980).

[5]G. Ciangaru, R. L. McGrath, and F. E. Cecil, Nucl. Phys. **A380**, 147 (1982); C. Gaarde, T. Kammuri, and F. Osterfeld, *ibid.* **A222**, 579 (1974).

[6]K.-I. Kubo, Nucl. Phys. **A246**, 246 (1975).

[7]S. H. Fox, and S. M. Austin, Phys. Rev. C **21**, 1133 (1980).

[8]T. N. Taddeucci, J. Rapaport, D. E. Bainum, C. D. Goodman, C. C. Foster, C. Gaarde, J. Larsen, C. A. Goulding, D. J. Horen, T. Masterson, and E. Sugarbaker, Phys. Rev. C **25**, 1094 (1982); J. A. Carr and F. Petrovich, private communication.

[9]A. Cunsolo, A. Foti, G. Imme, G. Pappalardo, G. Raciti, N. Saunier, and B. T. Kim, Nucl. Phys. **A355**, 261 (1981).

[10]F. W. Bingham, M. K. Brussel, and J. D. Steben, Nucl. Phys. **55**, 265 (1964).

[11]V. I. Chuev, V. V. Davidov, V. I. Manko, B. G. Novatsky, S. B. Sakuta, and D. N. Stepanov, Phys. Lett. **31B**, 624 (1970).

[12]M. F. Vineyard, J. Cook, K. W. Kemper, and M. N. Stephens, Phys. Rev. C **30**, 916 (1984).

[13]J. Cook, Comput. Phys. Commun. **31**, 363 (1984).

[14]K. W. Kemper, G. E. Moore, R. J. Puigh, and R. L. White, Phys. Rev. C **15**, 1726 (1977).

[15]P. D. Kunz (unpublished), with modifications by J. R. Comfort (unpublished).

[16]A. G. Blachman and A. Lurio, Phys. Rev. **153**, 164 (1967).

[17]H.-G. Clerc, K. J. Wetzel, and E. Spamer, Nucl. Phys. **A120**, 441 (1968).

[18]G. Bertsch, J. Borysowicz, H. McManus, and W. G. Love, Nucl. Phys. **A284**, 399 (1977).

[19]S. Cohen and D. Kurath, Nucl. Phys. **73**, 1 (1965); **A101**, 1 (1967).

[20]F. Petrovich, R. H. Howell, C. H. Poppe, S. M. Austin, and G. M. Crawley, Nucl. Phys. **A383**, 355 (1982).

[21]J. D. Anderson, C. Wong, and V. A. Madsen, Phys. Rev. Lett. **24**, 1074 (1970).

[22]F. Ajzenberg-Selove, Nucl. Phys. **A320**, 1 (1979).

[23]F. Ajzenberg-Selove, Nucl. Phys. **A360**, 1 (1981).

[24]A. W. Carpenter, private communication.

[25]W. M. Visscher and R. A. Ferrell, Phys. Rev. **107**, 781 (1957).

[26]P. D. Kunz (unpublished).